Conjugate momentum effects on the droplets heat transfer modeling calculated from the integral form of the Gamma distribution

Ahmed Abed Al-Kadhem Majhool[†*], Noor M. Jasim[‡]

[†] Department of Mechanical Engineering, Al-Qadisiyah University, Iraq.
[‡] Department of Mechanical Engineering, Kufa University, Iraq.

*Corresponding Author Email: ahmidkadhim@yahoo.com

ABSTRACT

In this work, it proposed an appropriate form of the droplets velocity formula in the integral form of the spray moment conservation equations, and coupling the effects of relative velocity term on the droplet heat transfer model in pressure-swirl atomized sprays. The spray tip penetration calculated in this approach agrees well with experimental data. The revised treatment of therm-physical properties of the liquid and gas phases also leads to quite stable calculations for a wide range of ambient temperatures and density ratios. The spray moments theory makes it possible to describe polydisperse sprays using an Eulerian approach and therefore appears to be a method indicated for two-phase evaporation applications. Its relevance for simulation at the scale of industrial applications is assessed in this work, by its implementation in two-dimensional configuration more representative of this type of pressure-swirl simulations. This evaluation couples a feasibility study in terms of calculation cost with an analysis of the precision obtained, by comparisons with the experimental data of reference methods for the description of sprays.

KEYWORDS

Spray modeling, Drop number size moments, Gamma distribution, Evaporation model, Droplet heating.

INTRODUCTION

Computational Fluid Dynamics (CFD), is representing a powerful tool in many applications industrial based on the motion of fluids, such as in the evaluation of work that the flow exchanges with the hot air, or in the determination of the thermodynamic properties of the droplets in the electrical field, but also in the analysis of the interactions between solid wall and wind. The physical processes involved in heating and evaporation are numerous and closely related. A droplet evaporating in the hot air is changing due to its temperature and composition. The variation is depending on the flows associated with evaporation, convective exchanges with the gas phase and thermal radiation to which it is subjected. Assuming, at each moment the thermodynamic equilibrium between the liquid phase and the gas phase in a thin film surrounding the drop, Raoult's law makes it possible to quantify the vapor fraction of each of the species as a function of the state of the phase liquid, pressure and temperature. In the case of an atmosphere unsaturated with vapor, at a temperature different from that of the drop, a thermal and mass gradient is established under the effect of diffusion. This gradient is responsible for setting the molecules in motion in the gas phase. In this configuration, the evaporation of the liquid components requires an input of energy taken from the liquid phase in the form of a flow thermal which induces a cooling of the drop.

The influence of the convective flow depends on the speed and on the temperature difference between the drop and the surrounding environment. In the event that the ambient temperature is higher, the convective flow induces a supply of heat to the drop. Knowing these flows at each moment determines the future state of droplet. The case of a multi-component drop is considered, composed of an ideal mixture of pure substances. Moreover, to predict the performance of a combustion chamber and in particular pollutant emissions, evaporation modeling

must also take into account the composition of the drop. The chemical description of combustion requires site to know precisely the species that burn, that is to say those that result from the evaporation of fuel. The distillation effect, which corresponds to the successive evaporation of species according to their volatility, can also modify the rate of evaporation. In the case of a mixture of components with very different physical properties, as in some new fuels, this can influence the coupling between the different physical phenomena. Thus, according to the richness of the medium in vapor, the position of the flame may for example be different. It is therefore interesting to have digital simulation tools capable of modeling the composition of the fuel.

Conventional models are too costly in computing time to be integrated directly into industrial-type computer codes. The second theme is thus devoted to the development of an evaporation model multi-component adapted, that to be used in the specific numerical methods. Models of evaporating fuel droplets are based on the assumption that fuels are single-component. To have a more realistic approach, it is necessary to get rid of this assumption. The study of the evaporation of multi-component droplets presents several complexities absent in simple analysis of a single-component drop: the boundary conditions and exchanges at the surface of the drop must be clearly defined for each component, the composition and temperature of the drop change continuously over time, the components do not all have the same volatility, they evaporate at different rates creating concentration gradients within the drop itself. The commonly used approach is based on the discrete component model, each one considered to be independent of the others [1, 2]. Generally, the thermodynamic equilibrium and the ideality of the mixtures are assumed at the surface of the drop according to Raoult's law.

Deviations from a ideal mixture can however be taken into account by introducing the parameter fugacity of the mixture [3,4]. This model is applicable for a fairly small number of components involved. Another approach to common fuels composed of hundreds of components is the so-called "continuous thermodynamics" approach; in this case, the properties of the components are represented by a continuous distribution function, which considerably limits the number of parameters [5]. The distribution variable can represent the molar mass or the number of carbon atoms. These models were first used in the field of chemistry to describe thermodynamic equilibrium [6]. This technique was then developed in the context of infinite diffusion or effective diffusion for modeling the evaporation of multi-component drops [7,8]. Hallett took inspiration from approach, which assumes that the probability density function associated with fuel composition is a function [6]. This model makes it possible to significantly reduce the calculation time, only the changes in the mean and the standard deviation of the function being calculated.

However, the description of the composition by an assumed function is not always relevant, as for example in the case where volatile species condense on the drop [9]. Many authors have shown the benefit of taking into account conduction in the liquid phase [10]. Various more or less complex models can be used to describe the transfer of species and heat in the liquid phase. The infinite diffusion model is based on the assumption of an infinitely rapid heat transfer inside the drop. It represents a borderline case for which the lifetime of the droplet is considered to be very long compared to the characteristic time of diffusion of heat and of the species in the liquid phase. Thus, the temperature and the composition of the liquid phase are spatially uniform but variable over time. This very simplified model has the advantage of being inexpensive in computing time. It is useful in order to obtain orders of magnitude on the phenomena of evaporation. The diffusion limit model developed by [1, 11]. This model assumes that there is no convective exchange within the drop.

The evolution of the composition and the temperature within the drop is purely radial and is governed by the unsteady equations of diffusion of species and of heat. Regarding the diffusion of heat inside the drop, one of the possibilities, in order to save calculation time, in particular by comparison to the complete resolution of the equation of heat in the drop, consists in assuming the shape of the profile of temperature inside the drop, while retaining axi-symmetry assumptions. Dombrovsky and Sazhin used a parabolic-type approximation for the temperature distribution over a radius of the drop [12]. The problem of droplet evaporation can appear relatively complex when all of the physical phenomena involved in the exchanges between the droplet and the gas phase are taken into account in the modeling. The presence of a boundary layer around the drop, of a wake and internal re-circulations induced by convective effects, can strongly modify these exchanges. The Reynolds number of the drop is therefore an important parameter in the models. The regression of the interface due to

evaporation, as well as the blowing of the boundary layer by the evaporated flow, are also phenomena that must be considered. This is why many empirical correlations are used in evaporation models.

The use of advanced numerical methods (Level-Set method, Ghost Fluid method), which make it possible to solve the problem of the evaporation of a drop by direct numerical simulation, are currently far too costly in computing time to consider replacing traditional models. However, they give the possibility of carrying out "digital experiments" very interesting to validate the models [13]. The description of classic multi-component evaporation models, called Discrete Component Models (or DCM for Discrete Component Model). An important work done in this part was to demonstrate the known results from the general conservation equations of mass, species and energy. In addition, the case of zero flow being singular for modeling and therefore critical for numerical simulations, a criterion making it possible to anticipate this case was highlighted, which made it possible to make the codes robust during the passage of a condensation regime with evaporation regime and vice versa. A detailed description of the conservation equations is given in [14].

The evaporation models are described by Sirignano, as well as in the work of Sezen [15, 16]. Finally, an interesting overview of the different models and their application is provided in a recent paper by Sazhin, which describes the issues associated with the modeling of evaporation, in particular concerning the themes of thermal conduction and the composition of the drops [17, 18]. In these models, the problem is assumed to be spherical symmetry, even when the drop is moving and this symmetry is broken (except in the case of the Hill Vortex model where the drop is treated in axial symmetry). The system is modeled by a drop surrounded by a boundary layer and the model equations are described in the referential linked to the drop. The terms of mass, species and heat transfer in the boundary layer are computed analytically while the equations of species and heat diffusion are solved numerically in the drop. Another approach studied by Singer, called the Moment Quadrature method (QmoM), makes it possible to overcome this difficulty, without making an assumption about the shape of the distribution function [19].

This approach is in a way a combination of the Discrete Component model and the so-called Continuous Thermodynamics model. Indeed, the distribution function used by this method is a sum of Dirac masses (as in the models with Discrete Components) but whose abscissas are variable over time (hence a Continuous Thermodynamic type description). In the case of the integration of multi-component evaporation models in industrial type calculation codes. The Moment Quadrature method has the advantage of being a method with certain interesting robustness properties [20]. The main intent of this paper is to model and consider the effect of coupling droplets momentum with the droplets averaged temperatures. The relevant correlations and equations used in the heat transfer model are derived in the next section. Subsequently the basic spray moments averaging method has been outlined for clarity. Many researchers studied and discussed the droplets and bubbles shape and size and flow patterns in multi-phase flow [21-28].

MATHEMATICAL MODEL

The method of moments is based on tracking the moments of the distribution, rather than following the distribution itself [29]. The precision of this method results in their conservation of the first three moments of the distribution, which physically represent the total number of droplets, their total diameter, and the total volume if the internal variable considered is the volume. The moments of the drop number probability distribution can be further simplified by using a moment transformation, are defined by:

$$M^{(k)} = \int_0^\infty D^k n(D) dD \tag{1}$$

where D is the diameter of the droplet and n(D) is the number of droplets. The moments of the transport velocity:

$$u^{(k)} = \frac{1}{M^k} \int_0^\infty D^k u(D) n(D) dD \tag{2}$$

Moments Model

$$\frac{\partial}{\partial t}(\rho_l M_1) + \frac{\partial}{\partial x}(\rho_l M_1 U_{l1}) = -S_{m1} \tag{3}$$

$$\frac{\partial}{\partial t}(\rho_l M_2) + \frac{\partial}{\partial x}(\rho_l M_2 U_{l2}) = -S_{m2} \tag{4}$$

$$\frac{\partial}{\partial t}(\rho_l M_3) + \frac{\partial}{\partial x}(\rho_l M_3 U_{l3}) = -S_{m3} \tag{5}$$

The balance of momentum over the domain of the dispersed phase is expressed in terms of for the moment-average liquid velocities and the mass-average velocity. The specific momentum of the liquid phase equations can be written in general form as:

$$\frac{\partial}{\partial t}(\rho_l M_1 U_{l1}) + \frac{\partial}{\partial x}(\rho_l M_1 U_{li} U_{l1}) = \frac{M_1}{Sc}\frac{\partial}{\partial x^2}(U_{li} + U_{l1}) - S_{U1} \tag{6}$$

$$\frac{\partial}{\partial t}(\rho_l M_2 U_{l2}) + \frac{\partial}{\partial x}(\rho_l M_2 U_{li} U_{l2}) = \frac{M_2}{Sc}\frac{\partial}{\partial x^2}(U_{li} + U_{l2}) - S_{U2} \tag{7}$$

$$\frac{\partial}{\partial t}(\rho_l M_3 U_{l3}) + \frac{\partial}{\partial x}(\rho_l M_3 U_{li} U_{l3}) = \frac{M_3}{Sc}\frac{\partial}{\partial x^2}(U_{li} + U_{l3}) - S_{U3} \tag{8}$$

The transport equation of the liquid phase energy equation can be expressed as:

$$\frac{\partial}{\partial t}(\rho_l M_1 h_{l1}) + \frac{\partial}{\partial x}(\rho_l M_1 h_{li} U_{l1}) = \frac{M_1}{Pr}\frac{\partial}{\partial x^2}(U_{li} + U_{l1}) - S_{h1} \tag{9}$$

$$\frac{\partial}{\partial t}(\rho_l M_2 h_{l2}) + \frac{\partial}{\partial x}(\rho_l M_2 h_{li} U_{l2}) = \frac{M_2}{Pr}\frac{\partial}{\partial x^2}(U_{li} + U_{l2}) - S_{h2} \tag{10}$$

$$\frac{\partial}{\partial t}(\rho_l M_3 h_{l3}) + \frac{\partial}{\partial x}(\rho_l M_3 h_{li} U_{l3}) = \frac{M_3}{Pr}\frac{\partial}{\partial x^2}(U_{li} + U_{l3}) - S_{h3} \tag{11}$$

where S is the source term of due to the inter-phase interactions with the gas phase. The gamma distribution is defined by:

$$n(D, x, t) = M_o \frac{(k+2)^k}{\Gamma(k)\, r_{32}} r^{k-1} e^{-(k+2)\frac{r}{r_{32}}} \tag{12}$$

and,

$$\Gamma(k) = \int_0^\infty x^{k-1} e^{-x} dx \tag{13}$$

where $\Gamma(k)$ is the gamma function and r_{32} is the Sauter mean radius of the number size distribution of the drops. This is defined by $r_{32} = M_3/M_2$. For numerical calculations, the gamma function can be approximated by [30]:

$$\Gamma(k) = \left(\left(\frac{k}{e}\left(k * \sinh\left(\frac{1}{k} + \frac{1}{810k^6}\right)\right)^{1/2}\right)^k\right)\left(\frac{2\pi}{k}\right)^{1/2} \tag{14}$$

with an error of at most 1% for values of k > 1.0. With three moments calculated through transport equations, there are two parameters ($M_3/M_2 = r_{32}$) and (M_2/M_1) available to determine r_{32} and k. Insertion of (3) into (2) and partial integration leads to:

$$M_i = \frac{(k+2)M_{i+1}}{(k+i)\, r_{32}} \tag{15}$$

hence, setting i=1,

$$k = \frac{2M_r - 1}{M_r - 1} \tag{16}$$

and,

$$M_r = \frac{M_2^2}{M_1 M_3} \tag{17}$$

Droplet heat transfer source terms

The one-dimensional droplet heat transfer is based on two assumptions in order to evaluate the droplet temperature. First the temperature distribution of the liquid spray is varying with the radial distance of the droplet. The second assumption is that a parabolic temperature profile is existing across any droplet [31]. The heat conduction model for droplet evaporation can be written as:

$$\frac{\partial T_l(r)}{\partial t} = \frac{\lambda}{cp_l \rho_l}\left(\frac{\partial^2 T_l(r)}{\partial r^2} + \frac{2}{r}\frac{\partial T_l(r)}{\partial r}\right) \tag{18}$$

where r is the droplet radius, _ is the droplet thermal conductivity. The boundary conditions for the above equation are

$$\dot{q}_{liquid} = \lambda_l \frac{\partial T_l(r)}{R_l \partial r} \quad , at\ r = r_s \tag{19}$$

$$\frac{\partial T_l(r)}{\partial r} = 0 \quad , at\ r = 0 \tag{20}$$

The parabolic profile of temperature can be written as

$$T_l(r) = a_T + b_T r + c_T r^2 \tag{21}$$

where a_T, b_T and c_T are the constants found from the boundary conditions, i.e.

$$\begin{cases} \frac{\partial T_l(r)}{\partial r} = 0 \quad , at\ r = 0 \\ T_l(r) = T^s \quad , at\ r = r_s \\ T^a \int_0^{r_s} r^2 dr = \int_0^{r_s} T(r)\ r^2 dr \end{cases} \tag{22}$$

According to equations (20) and (21), a_T, b_T and c_T can be evaluated as

$$\begin{cases} a_T = 0.5(5T^a - 3T^s) \\ b_T = 0 \\ c_T = 2.5(T^s - T^a) \end{cases} \tag{23}$$

Finally, equation (21) can be written as

$$T_i(r) = 0.5(5T^a - 3T^s) + 2.5(T^s - T^a)r^2 \tag{24}$$

The heat transferred by conduction into the drop is evaluated at the drop surface

$$\dot{Q}_{in,d} = \lambda_l A_s \frac{dT}{dr}\bigg|_{r=r_s} = 4\pi\lambda_l r_s^2 \frac{5(T^s - T^a)}{r_s} = 20\pi\lambda_l(T^s - T^a)r_s \tag{25}$$

where λ_l is the liquid thermal conductivity. The total heat transfer rate into all the spray drops locally is evaluated by integration over all the drops in a control volume by means of the number size distribution, hence,

$$\dot{Q}_{in} = \int_0^\infty Q_{in,d}\ n(r_s)dr_s = 20\pi\lambda_l \int_0^\infty (T^s - T^a)\ n(r_s)\ r_s dr_s \tag{26}$$

The surface liquid temperature T_{M2} and volume liquid temperature T_{M3} are outlined from the equations

$$T_{M2}M_1 = \int_0^\infty T^s\ r_s\ n(r_s)dr_s \tag{27}$$

and,

$$T_{M3}M_1 = \int_0^\infty T^a\ r_s\ n(r_s)dr_s = T^a M_1 \tag{28}$$

Thus, the liquid surface averaged temperature is expressed as

$$T_{M2} = T_{M3} + \frac{\dot{Q}_{in}}{20\pi\lambda_l M_1} \tag{29}$$

Hence once T_{M3} can be obtained from the liquid phase energy transport equation, T_{M2} can be evaluated, as long as Q_{in} can be found. The heat transfer between droplets and gas-phase is governed by the energy balance equation.

$$\dot{Q}_{cond} = 2\pi\lambda_g(T^g - T^s)Nu\frac{ln(1+B_M)^{1/Le}}{(1+B_M)^{1/Le}-1} \tag{30}$$

$$B_M \equiv \frac{f_s - f}{1 - f_s} \tag{31}$$

$$f_s = \frac{MW_d}{MW_d + MW_g(\frac{P_{total}}{P_{vap}} - 1)} \tag{32}$$

where,

$$f = \frac{\rho_m}{\rho_g} \tag{33}$$

where MW, P and ρ are the molecular weight, pressure and density respectively. The subscripts d, g and m refer to the droplet, gas and mixture respectively.

$$Nu = 2 + 0.6Re^{1/2}Pr^{1/3} \tag{34}$$

where Pr is the Prandtl number. The droplet velocity is assumed that the droplet velocity respond rapidly to the droplet radius, as follows:

$$U_l \propto r \tag{35}$$

Majhool et al. [32] proposed a relation that connected between droplet velocity and air is described by the relative velocity equation:

$$U_{rel} = U_l - v_g \tag{36}$$

Approximately, the droplet velocity is settled by the construction of a power relation between the droplet velocity and its diameter [14].

$$U_{rel} \approx \alpha r^\beta \tag{37}$$

The Reynolds number is defined for liquid droplets as

$$Re = \frac{2\rho_g U_{rel} r}{\mu_g} \tag{38}$$

By inserting equation (37) into (38)

$$Re = \frac{2\rho_g \alpha r^\beta r}{\mu_g} = \frac{2\rho_g \alpha r^{(1+\beta)}}{\mu_g} \tag{39}$$

The convective heat transfer rate must be equal to that entering the drop, therefore

$$Q_{in,d} = Q_{cond} \tag{40}$$

Thus, integration of (30), incorporating (34), over all droplets locally results in

$$\dot{Q}_{in,d} = 2\pi\lambda_l \int_0^\infty (T^g - T^s)\frac{ln(1+B_M)^{\frac{1}{Le}}}{(1+B_M)^{\frac{1}{Le}}-1}\left(2 + 0.6Re^{\frac{1}{2}}Pr^{\frac{1}{3}}\right)n(r_s)r_s dr_s \tag{41}$$

Substituted for Reynolds number using equation (39)

$$\dot{Q}_{in} = 2\pi\lambda_l \int_0^\infty (T^g - T^s)\frac{ln(1+B_M)^{\frac{1}{Le}}}{(1+B_M)^{\frac{1}{Le}}-1}\left(2 + 0.6(\frac{2\rho_g \alpha r^{(1+\beta)}}{\mu_g})^{\frac{1}{2}}Pr^{\frac{1}{3}}\right)n(r_s)r_s dr_s \tag{42}$$

Finally,

$$\dot{Q}_{in} = 2\pi\lambda_l \int_0^\infty (T^g - T^s) \frac{ln(1+B_M)^{\frac{1}{Le}}}{(1+B_M)^{\frac{1}{Le}-1}} \left(2M_1 + 0.6(\frac{2\rho_g\alpha}{\mu_g})^{\frac{1}{2}} M_{1.5+0.5\beta} Pr^{\frac{1}{3}} \right) \tag{43}$$

NUMERICAL METHODS

The simulations are calculated with the symmetric sector, as shown in Figure 1. The two-dimensional grid is created according to the dimensions of the one nozzle hole. As mentioned in the previous studies on spray penetration with evaporation, the unstructured grid has a cell side length of less than 0.1 mm. The initial simulation conditions for in-house code (spmom) are taken from Shim et al. [33] and Table 1 shows the operating conditions. The influence of the spray atomization with evaporation by the extended heat transfer model is examined. The turbulence model and the effects of the secondary breakup and the drop collision models are included more closely. To check the settings and models determined, the spray penetration is finally simulated and compared with the experimental data shim et al. [33]. The following simulation models are used. The Standard-k- model according to Launder and Spalding [34]. It is extended to the one-component fuel model. The Blob primary opening model by Reitz [35] and Kelvin-Helmholtz / Rayleigh-Taylor (KH / RT) secondary fracture model. The droplets collision model from O'Rourke [36]. The Spalding evaporation model with standard parameters [37]. The hexane fuel is used and the density and viscosity are adjusted according to the measurement data. A renewed investigation of the influence of the adaptation functions for viscosity and density is implemented, since these only influence the liquid phase or the breakup of the droplets. The computational domain for the hexane fuel spray is modeled by using an unstructured grid as shown in Figure 1a. The grid analysis is based on increasing grid density for the computational domain only at certain places as shown Figure 1b and Table 2 shows the grid specification.

Table 1. Experimental conditions taken from Shim et al.

| Fuel	Hexane
Injection Pressure (Mpa)	5.1
Injection duration (ms)	2.0
Injection quantity (mg)	15
Ambient gas	N_2
Ambient temperature (K)	9.3, 473
Ambient pressure (Mpa)	0.1
Impingement distance (mm)	46.7

Table 2. Grid specification.

Case	No. vol.	No. fac.	No. vert.	No. inj. cells
Case A	1906	3901	1996	5
Case B	1925	3939	2015	5
Case C	2011	4111	2101	5
Case D	2301	4317	2318	5
Case E	7799	15787	7989	5
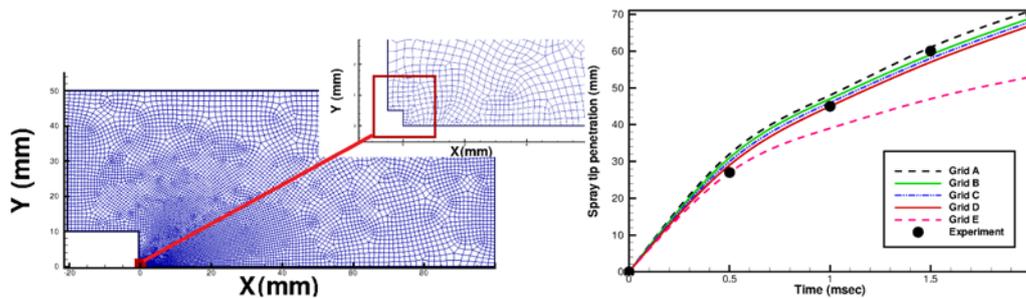
Figure 1. (a) Computational domain. (b) Spray tip penetration of with different number of control volumes.

RESULTS AND DISCUSSIONS

Figure 2 shows the predicated spray penetration versus time for the proposed model compared with experimental data at the ambient temperatures of 473 K. As the distance from the injection nozzle increases, the injected spray droplets are more and more dominated by the interaction between the injected fuel and the ambient gas in the test chamber. The cone angle of the spray, the area of interaction for the braking aerodynamic forces increase with increasing distance from the nozzle tip. The spray tip penetration has to move the gas in front of it, at the same time it consumes in a lot of gas from the surroundings in the rear area of the spray cone.
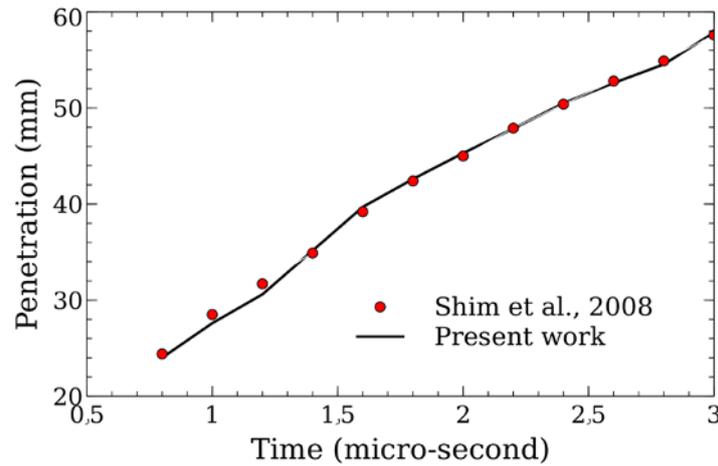

Figure 2. Comparisons of predicted spray penetration with experimental data of Shim et al. [33].

Figure 3 shows the droplet velocity distributions for the non-evaporating and evaporating cases. The figure explains the droplet velocity by size class of droplet. The velocity distribution curves are very close to the power law velocity profile. The droplet velocity by droplet size class also show similar trends for the two cases. This point is particularly interesting because, associated with the fact that the diameter distributions also seem to depend little on the injected liquid flow rate, they make it possible to expect fairly similar droplet characteristics regardless of the liquid flow rate used. The difference between them is as expected the evaporation process tends to reduce the liquid velocity along the axial distance due to consuming droplets.
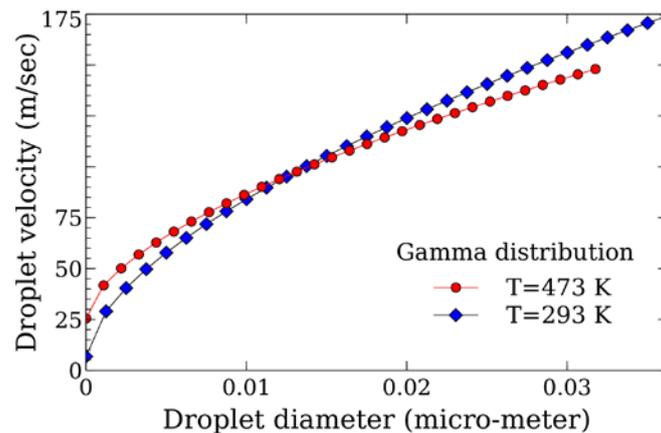

Figure 3. Comparison between droplet velocity at different ambient temperatures.

Figure 4 shows the distribution of the spray droplets of hexane to the axial position of 58 mm downstream of the injector seat, injection pressure of 5.1 MPa and ambient temperatures at 473K and 293K. The analysis of the droplet diameter distribution reveals some important characteristics of the spray behavior. A brief observation in Figure 4 demonstrates that the two curves of the tested fluid contain mono-modal shapes with small differences both in their centerlines and in their border regions due to the evaporation of droplets.
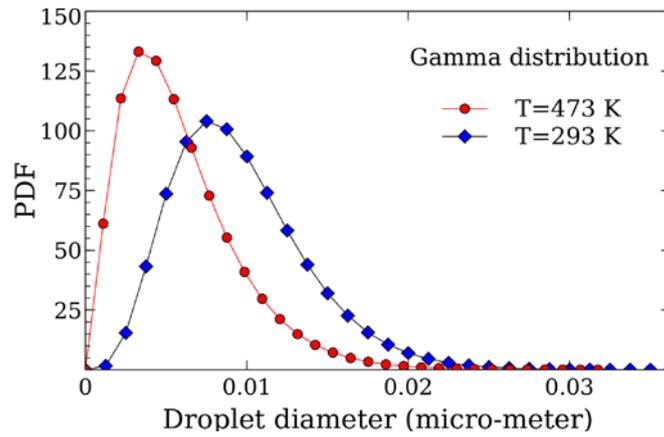
Figure 4. Comparison between drop size distribution at different ambient temperatures.

Figure 5 shows the axial and radial variation in the gas temperature at different times. It should be noticed that these profiles obtained by numerical simulation. The gas temperature is calculated at the central part of the hollow cone spray. This temperature is almost equal to the hot nitrogen injection temperature (approximately 473 K). Figure 5a shows the axial variation in the gas temperature at different times. It can be observed that the temperature does not remain constant it gradually decreases to a value of about 293 K near the injector. This decrease is due to the contact of the cold liquid droplets. The gas temperature values are increased as they move away from the axis of the spray. Figure 5b shows the radial variation in the gas temperature at different times. It can be seen that the gas temperature gradually decreases to a value of about 445 K at y=2 mm. This decrease is for the same reason, which is mentioned above. The gas temperature values are increased as they move away from the axis of the spray.
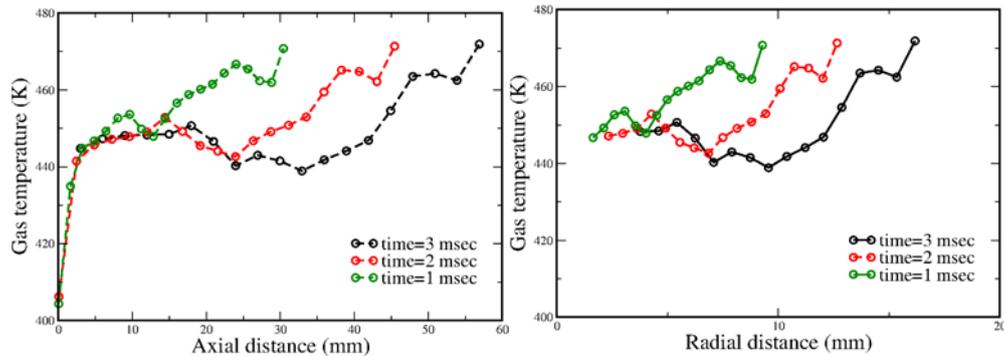

Figure 5. Radial and axial variation of gas temperature at different times.

In order to validate the evaporation model developed, the spray temperatures in a three zones are extracted. Figures 6 a & b show spray temperature at three zones downstream with axial and radial distances at time =2 msec. The first zone is the inner edge where the lowest temperatures are found. This is due to the less interaction between the core of the hollow cone spray with the hot gas. The second zone is the spray center. The highest values of droplet temperature are existed. The reason behind that is the presence of small droplets size that may evaporate faster than the bigger one that can be existed in the outer edge. Because of the centrifugal force the biggest droplets are moved the outer edge. The droplet with the higher mass has a high momentum (velocity) and tends to be at the rim of the cone.
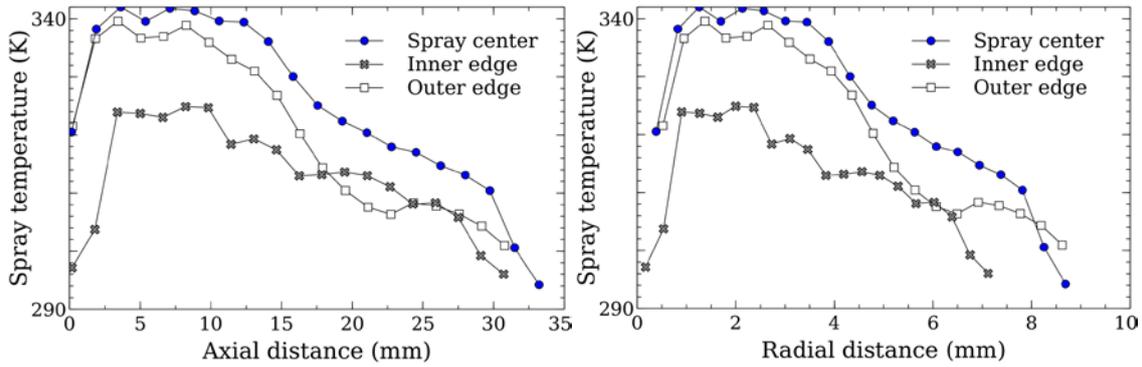
Figure 6. Radial and axial variation of spray temperature at different times.

The development of the hollow cone spray can be divided into two phases: the very short and transient phase at the beginning of the injection (pre-spray) and the steady-state phase corresponding to most of the injection duration. As the injection begins, a quantity of residual fuel from the injector that is trapped in the tangential slots (of swirl generation that are inside the injector), flows with velocity and the amount of angular movement and forms a kind of spray. This type of structure is typical of sprays generated by swirl type atomizers, such as the high-pressure swirl injector. Hollow cone with cone angle slightly wider than the angle of due to the main spray and large droplets, so it is called pre-spray. Figure 7a clearly shows the contour plot of this structure. As an example, Figure 7b shows the presence of point M that is selected on the outer edge of the spray. The point M is tracking the development of spray evaporation with time. With the 5.1 MPa injection, pressure and ambient back pressure 0.1 MPa.
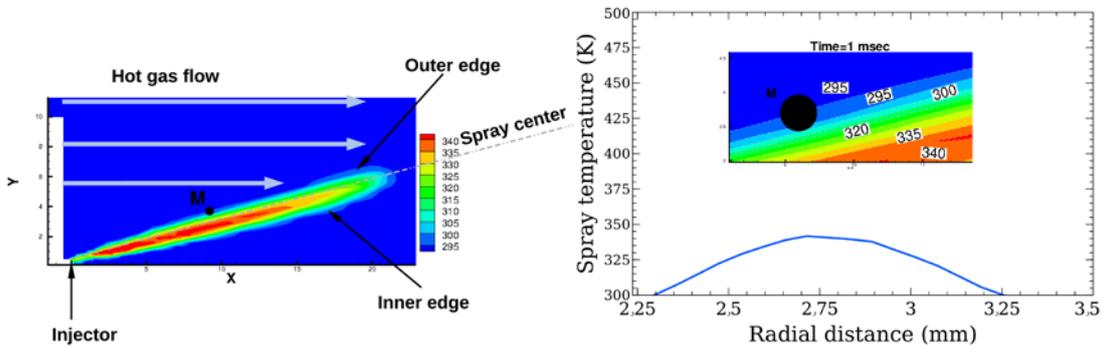
Figure 7. (a) Contour plot of spray temperature distribution; (b) Contour plot of spray temperature distribution at the outer edge.

Figure 8 shows the contour plot of a selected section of spray temperature at different times. The evaporation is a complex phenomenon as illustrated in the figure because it is including a coupling several thermodynamic (temperature, species, pressure) and dynamic (Stefan flux) variables. Another problem is involved, it arises from the characteristics of the hot ambient. The lifetime of a liquid droplets structure (the time required for the complete evaporation of this structure) is very long compared to the diffusion time of the vapor produced by evaporation. The lifetime of a drop is greater than the diffusion time by a factor at least equal to the density ratio of the two fluids considered. So, the area between the center of the spray and the outer edge is affected by the evaporation more than other zones.
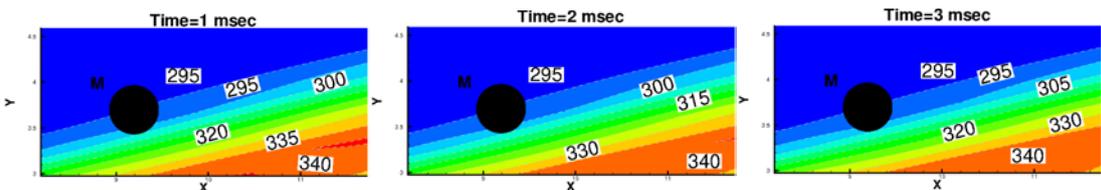
Figure 8. Contour plot of spray temperature distribution at the outer edge at different times.

CONCLUSION

This paper has described a derivation on the approach of spray moments theory, which is to extend a two-component evaporation model. It is adapted to high pressures and to implement it in the spmom code, has been achieved. The first step detailed the derived evaporation model of spmom and highlighted its weak points for use at high pressure. Following this analysis, it has developed a high pressure model with several improvements. Thus, the hypothesis of equality between the numbers of mass and heat transfers is no longer used and the numbers of Sherwood and Nusselt are now calculated using the Abramzon and Sirignano correlations. The calculations of phase equilibrium, interface composition and enthalpy of vaporization have been modified by the introduction of two new subroutines of the adaptation functions for liquid phase therm-physical properties. In particular, the Peng-Robinson cubic state equation is used and the thermodynamic equilibrium conditions are involved. The subroutine is calculating the physical properties of the liquid phase and gas phase. The effects of pressure and mixing vapor/ambient gas are taken into account through new correlations. Finally, it can be considered an extension of the evaporation model by introducing a model in terms of spray moments approach with multi zones inside the spray. This type of model makes it possible to take into account the thermal conduction and the scattering of the species in the phase.

REFERENCES

[1] W.A. Sirignano, "Fuel droplets vaporization and spray combustion theory", *Prog. Energy Combust. Sci.*, Vol. 9, Pp. 291-322, 1983.

[2] R.B. Landis and A.F. Mills, "Effect of internal resistance on the vaporization of binary droplets", *Fifth Int. Heat Transfer Conf., Tokyo, Japan*, B7-9, 1974.

[3] M. Burger, R. Schmehl, K. Prommerberger, O. Schfer, R. Koch and S. Wittig, "Droplet evaporation modelling by the distillation curve model: accounting for kerozene fuel at elevated pressures", *Int. J. Heat and Mass Transfer*, Vol. 46, Pp. 4403- 4412, 2003.

[4] S. Homann and U. Renz, "Numerical simulation of fuel sprays at high ambient pressure: the influence of real gas effects and gas solubility on droplet vaporization", *Int. J. Heat and Mass Transfer*, 46, Pp. 3017-3028, 2003.

[5] P. Le Clercq and J. Bellan, "Direct numerical simulation of a transitional temporal mixing layer laden with multi-component-fuel evaporating drop using continuous thermodynamics", *Phys. Fluids*, Pp. 1884-907, 2004.

[6] R.L. Cotterman, R. Bender and J.M. Prausnitz, "Phase equilibria for mixture containing very many components. Development and application of continuous thermodynamics for chemical process design", *Industrial and engineering Chemistry Process Design and Development*, Vol. 24, No. 1, Pp. 194-203, 1985.

[7] W.L.H. Hallet, "A simple model for the Vaporization of Droplets with Large Number of Components", *Combustion and flame*, Vol. 121, Pp. 334-344, 2000.

[8] Z. Abdel-Qader and W.L.H. Hallett, "The role of liquid mixing in evaporation of complex multicomponent mixtures: modelling using continuous thermodynamics", *Chemical Engineering Science*, Vol. 60, No. 6, Pp.1629-1640, 2005.

[9] K.G. Harstatd, P.C. Leclercq and J. Bellan, "Statistical model of multicomponent-fuel drop evaporation for many droplet flow simulations", *AIAA Journal,* Vol. 41, No. 10, Pp.1858-1874, 2003.

[10] C. Bertoli, M. Migliaccio, "A finite conductivity model for diesel spray evaporation computations", *Int. J. Heat Fluid Flow.*, Vol. 20, No. 5, Pp. 552561, 1999.

[11] R. Kneer, M. Schneider, B. Noll, and S. Wittig, "Diffusion controlled evaporation of a multicomponent droplet: theoretical studies on the importance of variable liquid properties", *Int. J. Heat Mass Transf.*, Vol. 36, No. 9, Pp. 24032415, 1993.

[12] L.A. Dombrovsky and S.S. Sazhin, "A parabolic temperature profile model for heating of droplets", Journal of heat transfer, 2003.

[13] S. Tanguy and A. Berlemont, "Application of a level set method for simulation of droplet collisions", *International Journal of Multiphase Flow,* Vol. 31, No. 9, Pp.1015-1035, 2005.

[14] K. Kuo, "Principles of Combustion", New York: John Wiley, 1986.

[15] W.A. Sirignano, "Fluid dynamics and transport of droplets and sprays", Cambridge University Press, 2010.

[16] Y. Sezen, "Unsteady mass transfer analysis of evaporation of a single multicomponent droplet with diffusion and constant rate processes", *International Communications in Heat and Mass Transfer*, Vol. 27, No. 4, Pp. 559-568, 2000.

[17] S.S. Sazhin, "Advanced models of fuel droplet heating and evaporation", *Progress in energy and combustion science*, Vol. 32, No. 2, Pp.162214, 2006.

[18] S.S. Sazhin, "Modelling of fuel droplet heating and evaporation: Recent results and unsolved problems", *Fuel,* Vol. 196, Pp. 69101, 2017.

[19] S.L. Singer, "Direct Quadrature Method of Moments with delumping for modeling multicomponent droplet vaporization", *International Journal of Heat and Mass Transfer*, Vol. 103, Pp. 940-954, 2016.

[20] A.Y. Cooney and S.L. Singer, "Modeling multicomponent fuel droplet vaporization with finite liquid diffusivity using Coupled Algebraic-DQMoM with delumping", *Fuel*, Vol. 212, Pp. 554-565, 2018.

[21] L.J. Habeeb and R.S. Al-Turaihi,"Experimental Study and CFD Simulation of Two-Phase Flow Around Triangular Obstacle in Enlarging Channel", *International Journal of Engineering Research and Applications (IJERA)*, Vol. 3, No. 4, Pp. 2036-2048, 2013.

[22] L.J. Habeeb and R.S. Al-Turaihi, "Experimental Study and CFD Simulation of Two-Phase Flow Around Multi- Shape Obstacles in Enlarging Channel", *American Journal of Mechanical Engineering (ajme) / Science and Education Publishing*, Vol. 1, No. 8, 470-486, 2013.

[23] L.J. Habeeb and R.S. Al-Turaihi," Steady and Unsteady Bubbly Two-Phase Flow (Gas-Liquid Flow) around a Hydrofoil in Enlarging Rectangular Channel", *International Journal of Computational Engineering Research*, Vol. 03, No. 9, Pp. 44-62, 2013.

[24] L.J. Habeeb, "Experimental and Numerical Study of Two-Phase Flow Regimes around a Circular Cylinder through Enlarging Channel", *The Iraqi Journal for Mechanical and Materials Engineering*, Vol. 14, No. 1, Pp. 129-144, 2014.

[25] I.M. Abed, R.H. Hameed and L.J. Habeeb, "Experimental Analysis of Two-Phase Flow Through Cylinderical Obstruction in Vertical Pipe", *International Journal of Mechanical Engineering and Technology (IJMET)*, Vol. 10, No. 01, Pp. 74–88, 2019.

[26] L.J. Habeeb, and H.S. Majdi, "Experimental and Numerical Studies of Two-Phase Flow in Ribbed Periodic Vertical Channel", *Journal of Advanced Research in Fluid Mechanics and Thermal Sciences,* Vol. 68, No. 1, Pp. 34-53, 2020.

[27] L.J. Habeeb, and H.S. Majdi, "Three-Phase Flow over Rectangular and Semicircular Ribbed Vertical Channel", *Journal of Mechanical Engineering Research and Developments*, Vol. 43, No. 6, Pp. 456-471, 2020.

[28] H.M.A. Hussein, S.T. Ahmed, and L.J. Habeeb, "Two-Phase Flow for Gas-Liquid, Gas-Solid, Liquid-Solid, And Liquid-Liquid in a Horizontal Smooth and Turbulator Conduit – A Review", *Journal of Mechanical Engineering Research and Developments*, Vol. 43, Pp. 26-50, 2020.

[29] J. Beck and A. Watkins, "On the Development of a Spray Model Based on Drop-Size Moments", *Proc. Roy. Soc. London, Ser. A: Math. Phys. Eng. Sci*. Vol. 459, Pp. 13651394, 2003.

[30] R.H. Windschitl, http://www.rskey.org/gamma.htm.

[31] A.P. Watkins, "Modelling the mean temperatures used for calculating heat and mass transfer in sprays," *International Journal of Heat and Fluid Flow*, Vol. 28, Pp. 388406, 2007.

[32] A.A. Majhool, N.H. Hamza and N.M. Jasim, "Spray Interface Drag Modeling Based on the Power-Law Droplet Velocity Using the Moment Theory", Journal of Applied Mechanics and Technical Physics, Vol. 61, Pp. 6169, 2020.

[33] Y.S. Shim, G.M. Choi and D.J. Kim, "Numerical modeling of hollow-cone fuel atomization, vaporization and wall impingement processes under high ambient temperatures", International Journal of Automotive Technology, Vol. 9, No. 3, Pp. 267275, 2008.

[34] B.E. Launder and D.B. Spalding, "Lectures in Mathematical Models of Turbulence Academic Press", London, England, 1972.

[35] D. Reitz and R. Diwakar, "Effect of drop breakup on fuel sprays", *SAE Technical Paper Series*, (860469), 1986.

[36] P.J. ORourke, "Collective Drop Effects on Vaporising Liquid Sprays", PhD Thesis, University of Princeton, 1981.

[37] A.A. Mostafa and H.C. Mongia, "On the modelling of turbulent evaporating sprays: Eulerian versus lagrangian approach", International Journal of Heat and Mass Transfer, Vol. 30, No. 12, Pp. 2583 2593, 1987.